Journal of Colloid and Interface Science 530 (2018) 37–45

Contents lists available at ScienceDirect

Journal of Colloid and Interface Science

journal homepage: www.elsevier.com/locate/jcis

Regular Article

Novel electrochemical synthesis of copper oxide nanoparticles decorated graphene-β-cyclodextrin composite for trace-level detection of antibiotic drug metronidazole

Vijayalakshmi Velusamy [a,*], Selvakumar Palanisamy [a,b], Thangavelu Kokulnathan [c], Shih-Wen Chen [b], Thomas C.K. Yang [b,*], Craig E. Banks [d], Sumit Kumar Pramanik [e]

[a] Division of Electrical, Electronic Engineering, School of Engineering, Manchester Metropolitan University, Manchester M1 5GD, United Kingdom
[b] Department of Chemical Engineering and Biotechnology, National Taipei University of Technology, No. 1, Section 3, Chung-Hsiao East Road, Taipei 106, Taiwan
[c] Electroanalysis and Bioelectrochemistry Lab, Department of Chemical Engineering and Biotechnology, National Taipei University of Technology, No. 1, Section 3, Chung-Hsiao East Road, Taipei 106, Taiwan
[d] School of Science and Environment, Manchester Metropolitan University, Chester Street, Manchester M1 5GD, United Kingdom
[e] CSIR-Central Salt & Marine Chemicals Research Institute, Bhavnagar 364 002, India

GRAPHICAL ABSTRACT

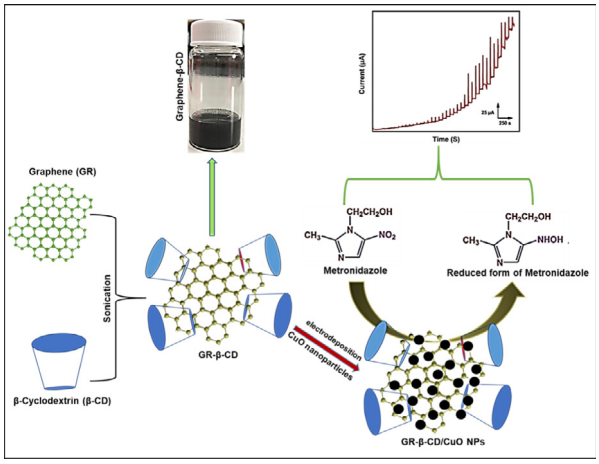

ARTICLE INFO

Article history:
Received 29 March 2018
Revised 20 June 2018
Accepted 21 June 2018
Available online 22 June 2018

Keywords:
Graphene
β-cyclodextrin
CuO
Electrochemical synthesis

ABSTRACT

Over the past decades, the synthesis of inorganic and organic nanocomposites has received much attention in the range of fields including electroanalysis of organic chemicals. In this regard, we have prepared copper oxide nanoparticle (CuO NPs) decorated graphene/β-cyclodextrin (GR-β-CD) composites using a simple electrochemical methodology, where the CuO NPs are electrodeposited on GR-β-CD composite modified electrodes. A stable GR-β-CD composite was prepared by sonication of GR in β-CD aqueous solution. As-prepared GR-β-CD/CuO NPs composites were characterized by the high-resolution scanning electron microscopy, X-ray diffraction, and Raman spectroscopy. Cyclic voltammetry results reveal that the GR-β-CD/CuO NPs composite modified electrode exhibits an excellent catalytic activity and lower reduction potential towards the electrochemical detection of metronidazole (MTZ) over other modified electrodes including GR, GR-β-CD, and CuO NPs. Under optimized conditions, amperometry was used for

* Corresponding authors.
E-mail addresses: V.Velusamy@mmu.ac.uk (V. Velusamy), ckyang@mail.ntut.edu.tw (T.C.K. Yang).

https://doi.org/10.1016/j.jcis.2018.06.056

Chemical sensor
Metronidazole

the determination of MTZ using GR-β-CD/CuO NPs composite modified electrodes. The response of MTZ using the composite electrodes was linear over the range from 0.002 to 210.0 μM. This sensor showed the lowest limit of detection of 0.6 nM and was much lower than the previously reported MTZ sensors. In addition, the sensor is highly sensitive, selective and durable in the presence of a range of potentially interfering electroactive compounds.

1. Introduction

Recent advancements of graphene-based composites have gained much attention in different applications including electrocatalysis [1]. Graphene (GR) has been widely known as a building block of all graphitic carbon forms, has a high theoretical surface area, mechanical strength and electrochemical activity over other carbon materials such as carbon nanotubes and C60 [2,3]. However, the stability of GR is poor in aqueous solutions due to the strong π-π stacking of individual GR sheets into graphite [4]. Henceforth, the different nano or micro materials including, but not limited to carbon nanomaterials [5,6], metal/metal alloy nanoparticles [7,8], supramolecular adducts [9], conducting polymer [10,11] and metal oxides [12,13] have all been used to prevent the π-π stacking of GR sheets. Furthermore, these GR based composites have shown an improved surface area and electrochemical activity over than of pristine GR. The GR based composites have also been used as an advanced electrode material for detection of toxic environmental pollutants in real systems [14–18]. Different polymer and nanomaterial supports have been used with GR to improve the dispersion ability and catalytic activity of GR. More recently, we have used β-cyclodextrin (β-CD) as a suitable dispersing agent for GR [19], which has dramatically improved the dispersion ability of GR in aqueous solution and prevent the re-stacking of GR sheets. Despite the exciting characteristics of β-CD (hydrophobic inner cavity and a hydrophilic exterior) that enables to form the stable composite with GR. In addition, the intercalation of unique properties of β-CD can enhance the catalytic activity of the GR. On the other hand, cupric oxide (CuO) has received significant attention in the scientific community due to its large surface to volume ratio and high catalytic activity and non-toxicity [20,21]. Despite these unique properties, CuO has been widely used in different applications including sensors [22], photocatalysis [23] and energy storage [24]. In comparison to other available methods, the electrodeposition of CuO has distinct advantages such as low operating temperatures and cost-effectiveness. In addition, the electrodeposition method can control the growth, morphology, structure, and orientation of CuO. Consequently, the integration of CuO with GR-β-CD composite could further improve the electrocatalytic activity of GR. Hence, in the present work, we have prepared CuO nanoparticle (CuO NPs) decorated GR-β-CD composites via a simple electrochemical methodology.

Metronidazole (MTZ) is an antibiotic drug and has been widely used for the treatment of pelvic inflammatory disease, endocarditis, and bacterial vaginosis [25,26]. However, the overdose and long-term use of MTZ will result in leucopenia, neutropenia, increased risk of peripheral neuropathy, and central nervous system toxicity [27]. Therefore, the accurate monitoring of MTZ concentrations in real samples is of significant interest. To date, the range of analytical methods has been used for the determination of MTZ such as high-performance liquid chromatography (HPLC), gas chromatography-mass spectrometry (GC–MS), liquid chromatography-mass spectrometry (LC-MS) and electrochemical methods. In comparison with available spectrophotometry and chromatography traditional methods [28], electrochemical methods are found to be simple and cost-effective and offer more sensitivity and selectivity towards the determination of MTZ [29]. Unmodified graphite or glassy carbon electrodes are not suitable for determination of MTZ due to their low sensitivity, low selectivity and fowling or drifting of electrochemical signals. Hence, different micro or nanomaterial-modified electrodes have been used for the sensitive and selective detection of MTZ [30]. In the present work, the as-prepared GR-β-CD/CuO NPs composite was used as a sensitive and lower potential electrode material for detection of MTZ for the first time. In addition, a simple electrochemical method was used for the decoration of CuO NPs on pristine GR-β-CD composite modified glassy carbon electrode (GCE).

2. Experimental section

2.1. Materials

Graphene nanoflakes (thickness = 8 nm) and metronidazole (analytical standard) were purchased from Sigma-Aldrich. β-cyclodextrin, $CuCl_2$, KCl and other chemicals were obtained from Sigma-Aldrich. All chemicals were of standard analytical grade and used as received. The stock solutions and electrolyte solutions were prepared using double distilled (DD) water without any further purification. The pH 7.0 (phosphate buffer) was used as a supporting electrolyte, and was prepared using 0.1 M Na_2HPO_4 and NaH_2PO_4 in DD water. The pH of the solution was adjusted using either 0.1 M NaOH or diluted H_2SO_4. DC150H Ultrasonicator from Taiwan Delta New Instrument Co. Ltd. with an operating frequency of 40 kHz and ultrasonic power output of 150 W was used for sonication.

2.2. Characterization methods

High-resolution scanning electron microscopic (SEM) images were taken by Hitachi S-4300SE/N High-Resolution Schottky Analytical VP electron microscope. The elemental spectral analysis (EDS) of the GR-β-CD/CuO NPs composite was analyzed using BRUKER AXS elemental analyzer with Hitachi S-4300SE/N High-Resolution Schottky Analytical VP SEM. The Zetasizer Nano ZS90 (Malvern Panalytical) was used for the Zeta potential and hydraulic diameter measurements. Raman spectrum was acquired by a Dong Woo 500i Raman spectrometer from Korea. X-ray diffraction (XRD) analysis was performed using XPERT-PRO diffractometer from PANalytical B.V., The Netherlands.

2.3. Electrochemical measurements

Cyclic voltammetry and amperometry experiments were performed using CH750A electrochemical workstation from CH Instruments, USA. GR-β-CD/CuO NPs composite modified GCE (the geometric surface area = 0.8 cm^2) was used as a working electrode, and saturated Ag/AgCl and a platinum wire were used as the reference and auxiliary electrodes, respectively. The electrochemical measurements were carried out at room temperature in an N_2 atmosphere unless otherwise stated.

2.4. Sensor fabrication

First, GR-β-CD composites were prepared via our previous reported methodology [19]. Briefly, 5 mg of GR nanoflakes were added into β-CD (5 mg mL^{-1}) aqueous solution via sonication of ~30 min at room temperature. 8 μL of the as-prepared GR-β-CD composite were dropped onto pre-cleaned GCE and dried at room temperature. For the electrodeposition of CuO NPs, 0.1 M $CuCl_2$ and 0.1 M KCl were prepared in a 20 mL electrochemical cell and the pH of the solution adjusted to 11 using NaOH. Then, the GR-β-CD composite modified GCE was immersed into the electrochemical cell, and 20 cyclic voltammetry cycles were performed in the potential sweeping from +1.1 to −0.7 V at a scan rate of 50 mV/s [31]. The resulting CuO NPs decorated GR-β-CD composite modified GCE was dried in an air oven for 5 min. For comparison, CuO NPs modified electrodes was prepared by a similar procedure without GR-β-CD composite. The GR and GR-β-CD composite modified GCEs were prepared without electrodeposition of CuO NPs, where 8 μL of GR and GR-β-CD composite dispersions were drop coated on GCE. The GR dispersion was prepared by dispersing of 5 mg GR nanoflakes in 1 mL dimethylformamide for sonication about 30 min. All fabricated modified electrodes were stored at room temperature under a dry condition when not in use.

3. Results and discussion

3.1. Characterization of GR-β-CD/CuO NPs composite

The surface morphology of as-prepared materials were characterized by SEM, and the SEM images of as-prepared CuO NPs, GR, GR-β-CD and GR-β-CD/CuO NPs composite are shown in Fig. 1. The SEM image of electrodeposited CuO (A) shows a uniform distribution of nano-sized particles, and the diameter of nanoparticles were in the range between 40 and 90 nm. The SEM of GR (B) shows its unique ultra-thin sheet-like morphology, while the GR-β-CD composite (C) shows a crumbled morphology wherein the GR nanosheets were enfolded by β-CD [19]. On the other hand, a uniform sized CuO NPs are clearly visible on the crumbled surface of the GR-β-CD composite from the SEM images of Fig. 1D. Furthermore, the diameter of the electrodeposited CuO NPs on GR-β-CD composite was in the range from 45 to 80 nm, and is more consistent with the SEM image of CuO NPs. The strong film-forming ability of GR and the host-guest interaction of β-CD with CuO NPs are resulting into the formation of homogenous morphology and less agglomeration of CuO NPs on GR-β-CD composite. The EDS was used to confirm the presence of copper, carbon, and oxygen in GR-β-CD/CuO NPs composite. As shown in Fig. 2A, the strong signal of carbon, oxygen and copper was observed for the EDS of GR-β-CD/CuO NPs composite. The result confirms the presence of carbon, oxygen and copper in GR-β-CD/CuO NPs composite. The Zeta potentials of CuO NPs and GR-β-CD/CuO NPs composite was measured to study the stability and charge of the synthesized CuO NPs in pH 7.0. The obtained Zeta potential distribution results are shown in Fig. 2B and C. The Zeta potential of the electrodeposited CuO NPs was +2.2 mV, which indicates that the CuO NPs are slightly positively charged in pH 7.0. However, the Zeta potential of GR-β-CD/CuO NPs composite was found to be −34.5 mV, which reveals the negatively charged nature of the fabricated composite in pH 7.0. It worthy to note that the CuO NPs are highly stable on the GR-β-CD composite in pH 7.0 rather than CuO NPs in pH 7.0. The dynamic light scattering measurements shows that the average hydraulic diameter of pristine CuO NPs and CuO NPs on GR-β-CD/CuO NPs composite was 117.1 nm (97.3% intensity) and 90.6 nm (99.2% intensity), respectively. The observed hydraulic diameter of CuO NPs is higher than those observed in SEM (Fig. 1A and D), which shows the agglomeration of CuO NPs in pH 7.0. However, the GR-β-CD composite improved the stability of CuO NPs and prevented the agglomeration of NPs in pH 7.0.

XRD and Raman spectroscopy was also used to confirm the formation of the GR-β-CD/CuO NPs composite and purity of utilized GR. Fig. 3A depicts the XRD pattern of as-prepared GR-β-CD/CuO NPs composite. The diffraction pattern shows the main characteristic peaks for (0 0 2) plane centered of GR at $2\theta = 22.6°$ and a weak peak at $2\theta = 40°$ for crystal plane for GR [32]. Five main

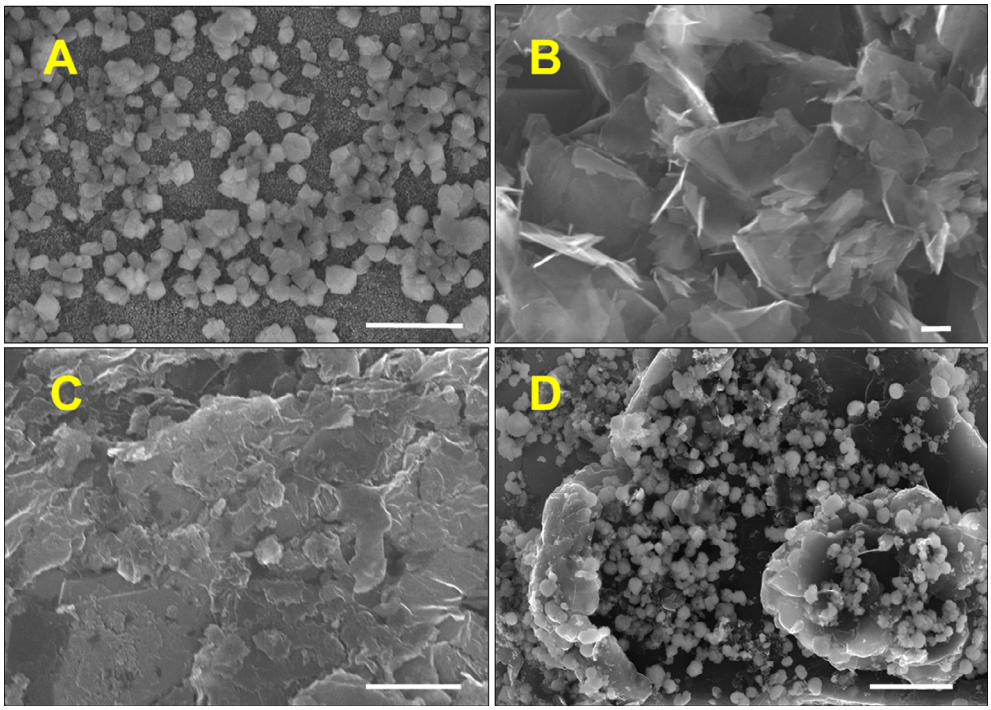

Fig. 1. High-resolution SEM images of CuO NPs (A), GR (B), GR-β-CD (C) and GR-β-CD/CuO NPs composite (D). Scale bar = 1 μm.

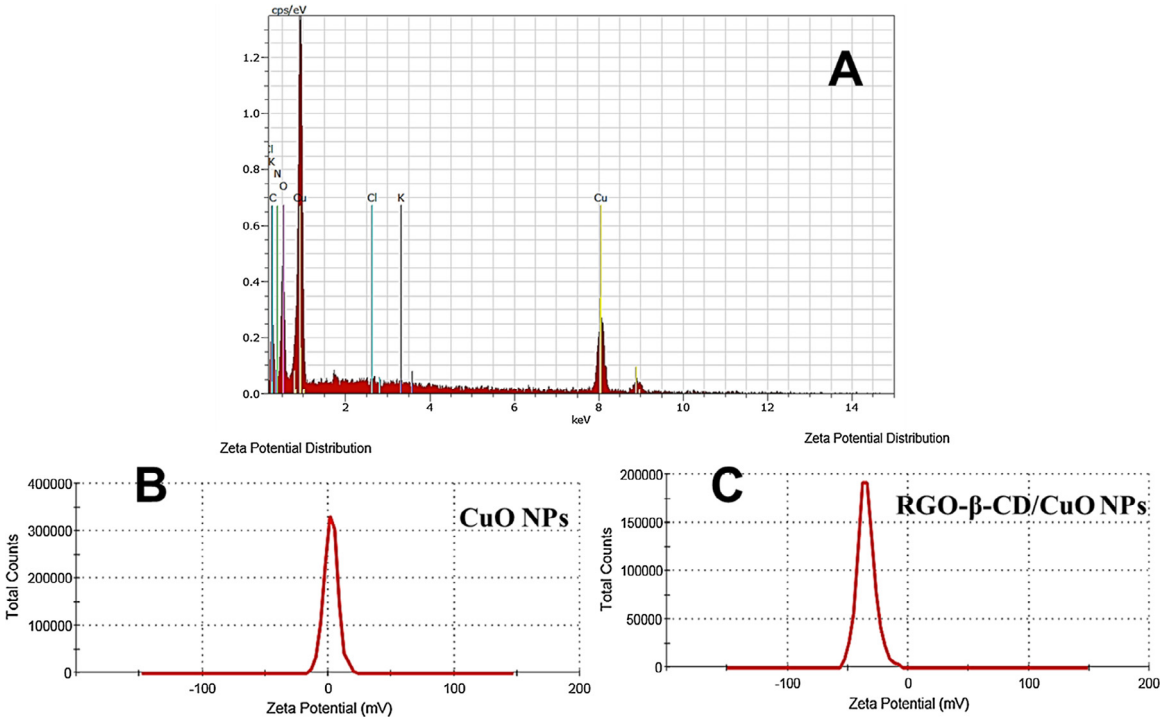

Fig. 2. (A) EDS of as-prepared GR-β-CD/CuO NPs composite. Zeta potential distribution for CuO NPs (B) and GR-β-CD/CuO NPs composite (C) in pH 7.0.

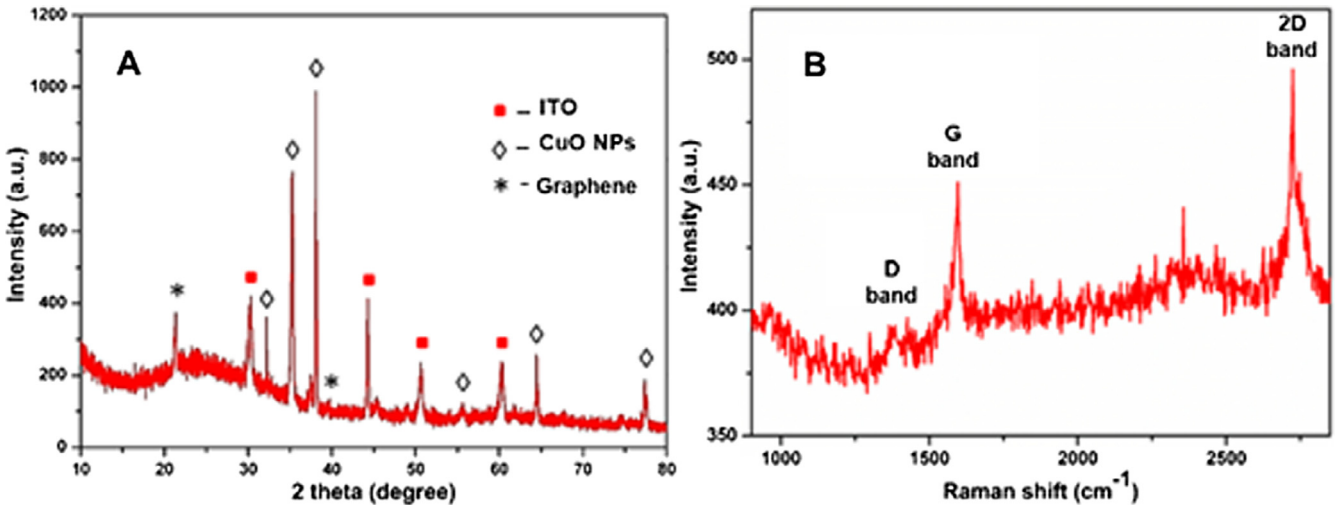

Fig. 3. (A) XRD pattern and Raman spectrum (B) of GR-β-CD/CuO NPs composite.

characteristic peaks of CuO appeared at 32.7°, 36.1°, 38.6°, 54.4°, and 65.3° corresponding to Miller indices (1 1 0), (0 0 2), (1 1 1), (0 2 0) and (2 2 0), respectively [33]. The characteristic peak at 73.5° is due to the reflections of (3 1 1) crystal plane of Cu_2O. The other reflection peaks are due to the presence of base indium tin oxide (ITO) electrode. Raman spectroscopy was also used to study the defects and purity of utilized GR in the composite and corresponding Raman spectrum is shown in Fig. 3B. The Raman spectrum GR shows the two distinct characteristic peaks in 1580 and 2721 cm^{-1}, is resulting from the presence of G and 2D band of graphene [34,35]. The G/2D intensity ratio was 0.9, which shows the utilized GR contain few-layered GR, which is consistent with our previous report [36].

3.2. Electrochemical behavior of MTZ at different modified electrodes

Cyclic voltammetry was used to evaluate the electrochemical behavior of MTZ at different modified electrodes. The electrochemical behavior of different electrodes such as unmodified GCE, and GR, GR-β-CD, CuO NPs and GR-β-CD/CuO NPs composite modified GCEs were studied in pH 7.0 containing 50 μM MTZ. The cyclic voltammetry experiments were performed over the potential range of 0.2 to −1.0 V at a scan rate of 50 mV/s. As shown in Fig. 4A, the bare (curve a) and CuO NPs (curve b) modified electrodes show a distinct reduction peak at −0.786 and −0.768 V for the presence of MTZ. The reduction peak is attributed to the direct electrochemical reduction of the nitro group of MTZ to the

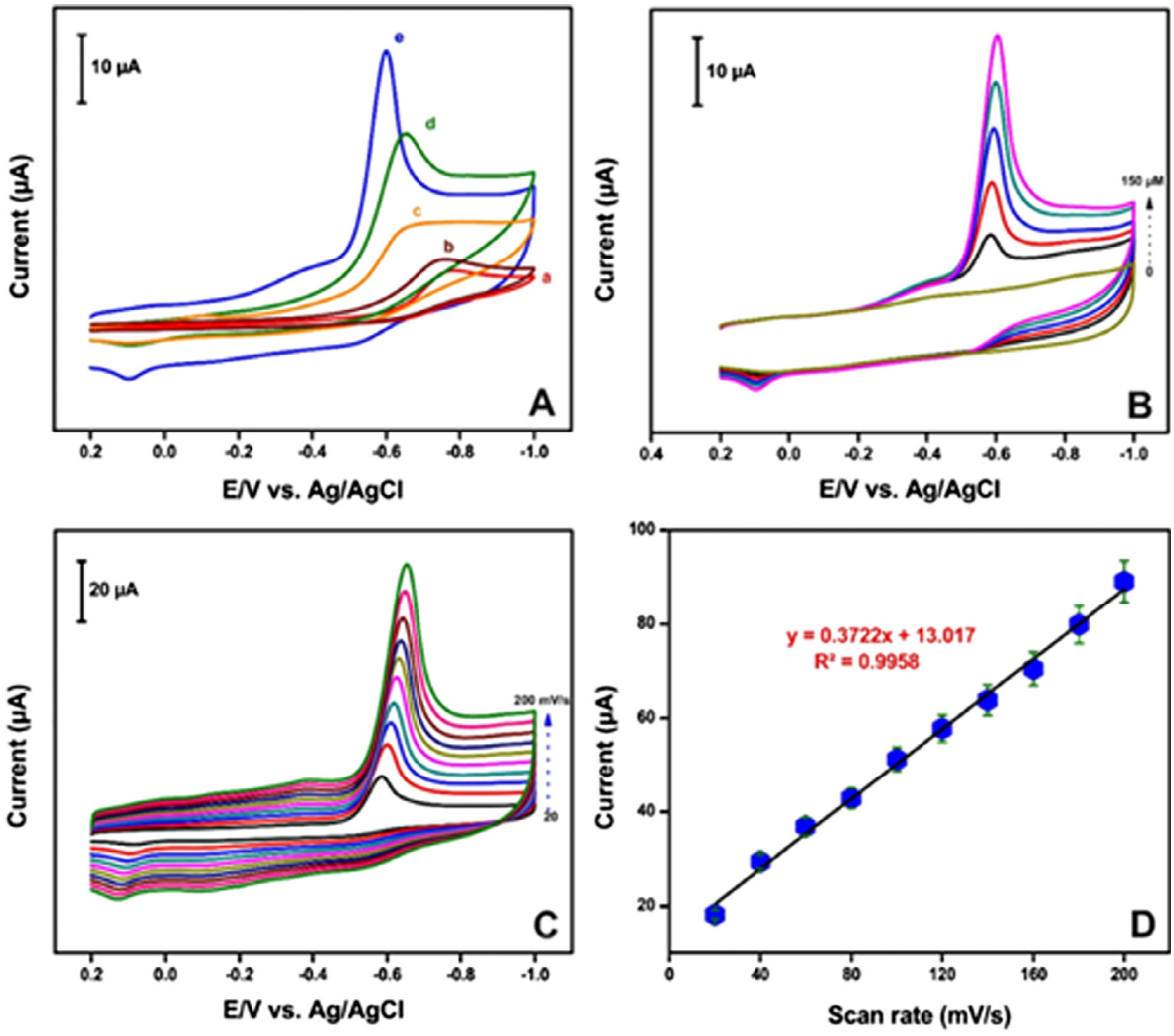

Fig. 4. (A) Cyclic voltammetry response of (a) bare, (b) CuO NPs, (c) GR, (d) GR-β-CD and (e) GR-β-CD/CuO NPs modified electrodes in the presence of 50 µM MTZ containing N_2 saturated pH 7.0 at a scan rate of 50 mV/s. (B) Cyclic voltammetry response of GR-β-CD/CuO NPs modified electrode in the absence and presence of different concentrations (10–50 µM) of MTZ in pH 7.0 at a scan rate of 50 mV/s. (C) Cyclic voltammetry response of 50 µM MTZ at GR-β-CD/CuO NPs modified electrode with different scan rates (20–200 mV/s) in pH 7.0. (D) The calibration plot of peak current vs. scan rate.

corresponding hydroxylamine. The reduction peak/signal of the MTZ is observed to be significantly enhanced using the GCE modified with GR (curve c). In addition, the reduction peak potential is observed to decrease to −0.642 V from −0.786 V, and is observed to be 144 and 126 mV lower than that of the bare and CuO NPs modified GCEs. The result shows that the electro-reduction ability of MTZ enhanced in GR modified electrode and is due to the larger surface area and high electron conducting nature of GR. On the other hand, the reduction peak current response to MTZ further enhanced (curve d) upon introduction of β-CD with GR (GR-β-CD modified electrode), which is due to the unique combined properties of GR (higher surface area) and β-CD (high-adsorption ability). However, the reduction peak potential of MTZ at GR-β-CD electrode found same as observed at GR modified electrode. The result clearly shows that the enhanced reduction peak current is clearly due to the high adsorption capability of β-CD towards MTZ. The GR-β-CD/CuO NPs composite modified electrode (curve e) shows 1.2, and 3 fold enhanced current response to MTZ than GR-β-CD/ and GR modified electrodes. In addition, the reduction potential of MTZ at GR-β-CD/CuO NPs composite modified electrode appears at −0.596 V. The observed reduction peak potential of MTZ at GR-β-CD/CuO NPs composite modified electrode was 48 mV lower than GR and GR-β-CD modified electrodes. The enhanced current response and lower reduction potential of MTZ at GR-β-CD/CuO NPs composite modified electrode is possibly due to the presence of combined unique properties (high surface area and adsorption ability) of GR-β-CD and CuO NPs. The result also confirms that GR-β-CD/CuO NPs composite modified electrode can be used for the sensitive and lower potential detection of MTZ over the other modified electrodes such as CuO NPs, GR, and GR-β-CD composite.

3.3. Effect of scan rate and pH

Cyclic voltammetry was used to explore the electrocatalytic ability of the GR-β-CD/CuO NPs composites towards the sensing of MTZ. Fig. 4B shows the cyclic voltammetry response of GR-β-CD/CuO NPs composite modified GCE in N_2 saturated pH 7.0 in the absence and presence (10–50 µM) of MTZ at a scan rate of 50 mV/s. In the absence of MTZ, GR-β-CD/CuO NPs composite modified electrode did not show any obvious response, which indicates that the composite modified electrode is electrochemically inactive in pH 7.0 at this scanned potential window. Whereas, a well-defined reduction peak was observed at −0.592 V for the presence of 10 µM MTZ. The reduction peak current response increases with

the further additions of MTZ into the pH 7.0. The result authenticates that GR-β-CD/CuO NPs composite modified electrodes have a useful electrocatalytic activity towards the reduction of MTZ. To understand the electrochemical behavior of MTZ at GR-β-CD/CuO NPs composite modified electrode, the effect of scan rate was studied using cyclic voltammetry. Fig. 4C shows the cyclic voltammetry response of GR-β-CD/CuO NPs composite modified electrode in 50 μM MTZ containing pH 7.0 at different scan rates from 20 to 200 mV/s. It can be seen that the reduction peak current response of MTZ increases with increasing the scan rate from 20 to 200 mV/s. In addition, a notable shift in the reduction peak potential of MTZ was observed upon increasing the scan rate from 20 to 200 mV/s. As shown in Fig. 3D, the scan rate was linearly proportional to the cathodic peak current response of MTZ with the correlation coefficient (R^2) of 0.9958. The result confirms that the electrochemical behavior of MTZ at the composite modified electrode was typically adsorption-controlled electrochemical process [36].

The effect of pH was studied using the cyclic voltammetry, and it can provide useful information to calculate the number of electrons and protons involved in the electrochemical reduction. Fig. 5A shows the cyclic voltammetry response of GR-β-CD/CuO NPs composite modified electrode in 50 μM MTZ containing various pH at a scan rate of 50 mV/s. It can be seen that a well-defined reduction peak was observed for MTZ in each pH and the reduction peak shifted towards negative direction upon increasing the pH from 7.0 to 11.0. The positive shift in reduction peak was observed when the pH was decreasing pH 7.0–3.0. The phenomenon indicates that the protons were involved in the reduction of MTZ. A linear plot has made for peak current versus pH, and corresponding calibration plot is shown in Fig. 5B. It can be seen that the reduction peak potential of MTZ had a linear relationship with the pH, and the slope was 0.9912. Fig. 5B also confirmed that a maximum reduction peak current response of MTZ was obtained at pH 7.0. One can see that the reduction peak current of MTZ decreased when the pH was below or above pH 7.0 (blue denotation). The result also confirms that pH 7.0 is an optimum for more sensitivity and hence pH 7.0 was used for further experimental studies. The possible electrochemical reduction mechanism of MTZ at the GR-β-CD/CuO NPs composite modified electrode is shown in Fig. 6.

3.4. Amperometric determination of MTZ

Amperometry was used for the quantification of MTZ using the GR-β-CD/CuO NPs composite modified electrode. Rotating disc electrode (RDE) with a surface area of 0.8 cm^2 was used for amperometric measurements. Amperograms of the composite electrode for MTZ was obtained in a constantly stirred (900 RPM) pH 7.0 at a working potential of −0.6 V. Fig. 7A shows the typical amperometric i-t response of GR-β-CD/CuO NPs composite modified RDE for different concentration additions of MTZ (2 nM–210.0 μM) into the pH 7.0. It can be seen that a sharp amperometric response was observed for the addition of 2, 10, 50, 100, 500, 1000 nM of MTZ (first 6 amperometric curves) into the pH 7 and the response current increases with increasing the addition of MTZ concentration (5 and 10 μM). The amperometric response current increases with the addition of MTZ from 2 nM to 210.0 μM, and the response time of the sensor was 3 s. The result demonstrates that GR-β-CD/CuO NPs composite modified electrode has fast electrocatalytic reduction towards MTZ. As shown in Fig. 7B, the amperometric response of the GR-β-CD/CuO NPs composite modified electrode was linear over the concentration of MTZ from 2 nM to 210.0 μM with the R^2 of 0.9969. The limit of detection (LOD) of the sensor was

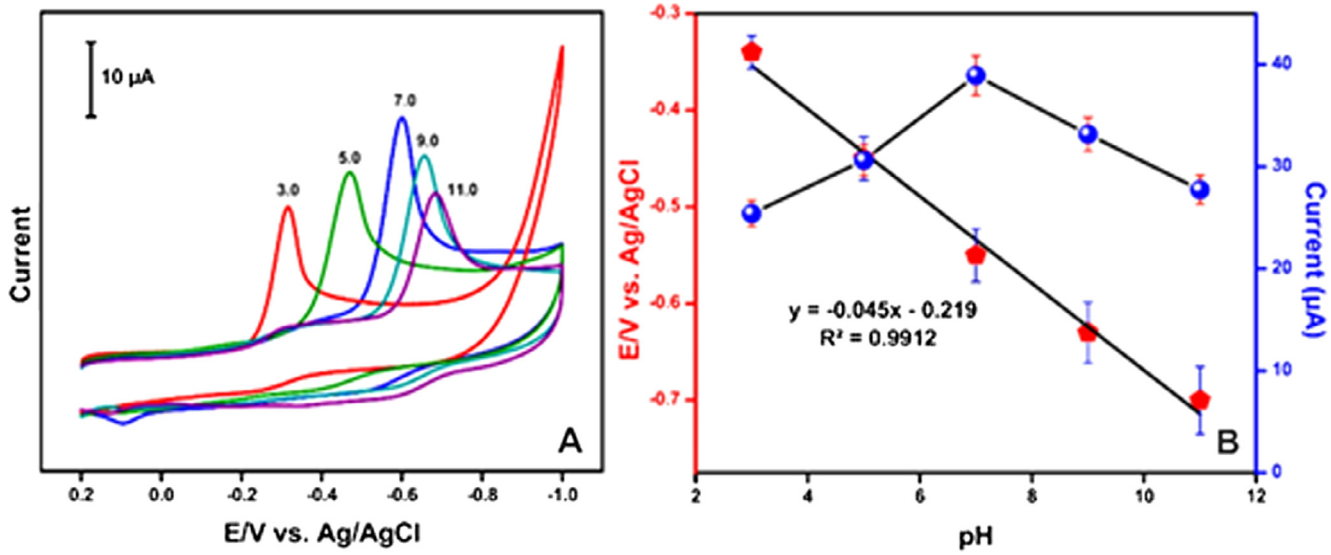

Fig. 5. (A) Cyclic voltammetry response of GR-β-CD/CuO NPs modified electrode in 50 μM MTZ containing different pH (pH 3.0–11.0) at a scan rate of 50 mV/s. (B) The linear plot for pH vs. reduction peak potential (red denotation) and reduction peak current (blue denotation). (For interpretation of the references to colour in this figure legend, the reader is referred to the web version of this article.)

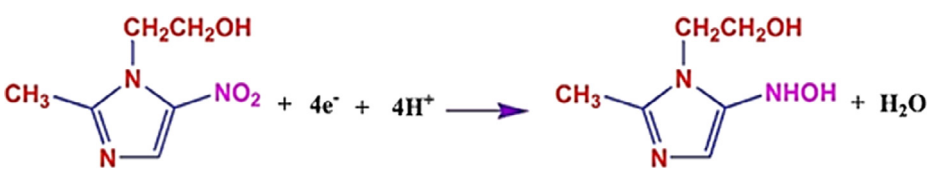

Fig. 6. Possible electrochemical reduction mechanism of MTZ at GR-β-CD/CuO NPs composite.

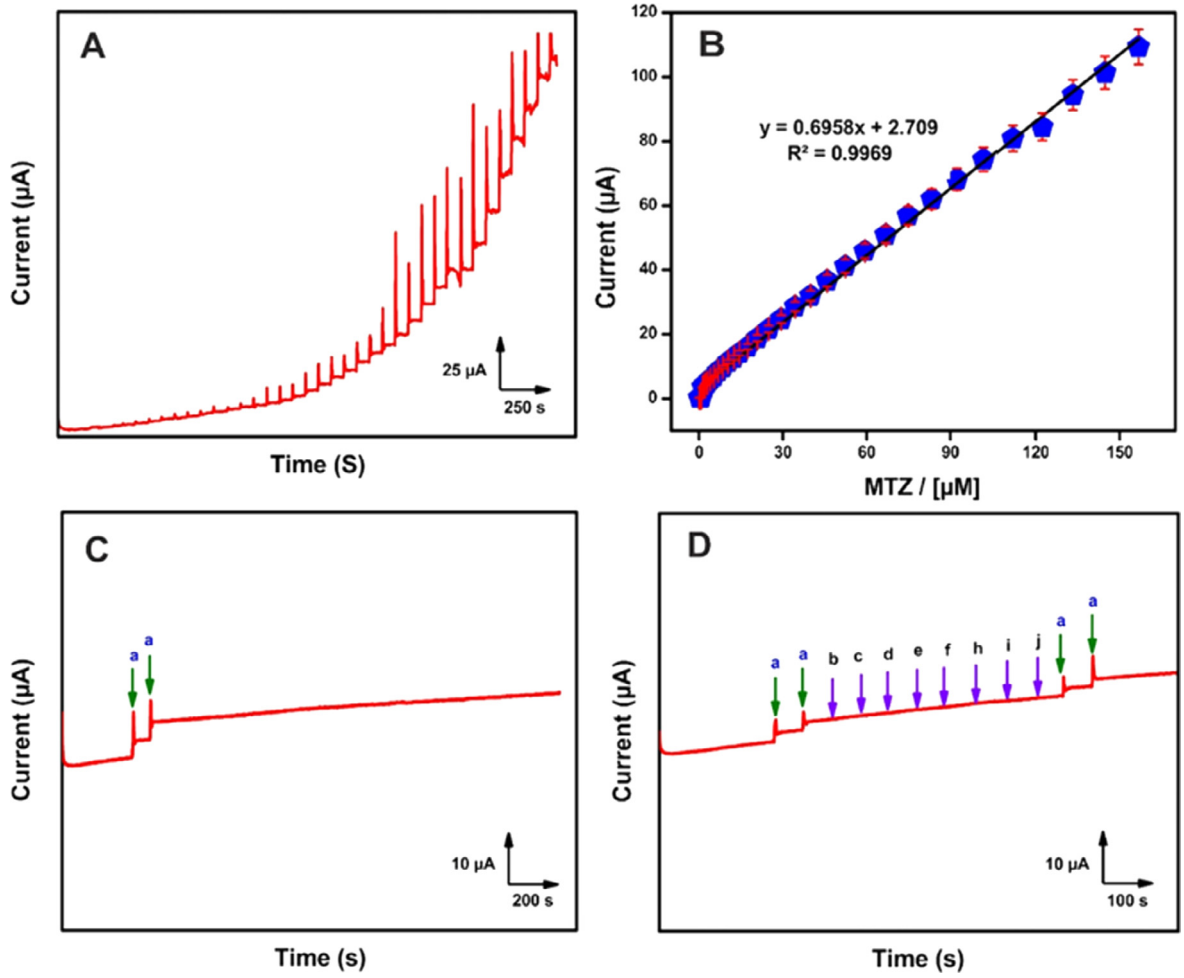

Fig. 7. (A) Amperometric response of GR-β-CD/CuO NPs composite modified RDE upon successive addition of various concentration of MTZ (0.002–210.0 μM) into N_2 saturated pH 7.0. Working potential = −0.6 V. (B) The calibration curve for [MTZ] vs. amperometric current. (C) Amperometric response of GR-β-CD/CuO NPs composite modified RDE for the addition of 500 nM MTZ (a) and the current background response up to 2000 s. (D) Amperometric response of GR-β-CD/CuO NPs composite modified RDE for addition of 50 nM MTZ (a) and 20-fold additions of (b) 4-nitrophenol, (c) nitrobenzene, (d) nilutamide, (e) glucose, (f) dopamine, (g) glutaric acid, (h) serotonin, (i) histidine and (j) flutamide.

estimated as 0.6 nM based on 3 ∗ Sd of the blank response/slope of the calibration plot. The sensitivity of the sensor was 0.7 $\mu A \mu M^{-1}$ and was calculated from the slope of the calibration plot. To verify the novelty and advantage of the GR-β-CD/CuO NPs composite modified electrode, the obtained analytical features (linear response range, $R^{2,}$ and LOD) were compared with previously reported MTZ sensors. The comparative results are shown in Table 1. The comparative results reveal that the LOD of the fabricated sensor (0.6 nM) is much lower than previously reported MTZ sensors such as graphene-ionic liquid/GCE (47.0 nM) [30], activated GCE (1.1 μM) [37], multiwalled carbon nanotubes/GCE (6 nM) [38], single wall carbon nanotubes/GCE (63.0 nM) [39], gold electrode (157.0 nM) and silver nanoparticles/sulfonate functionalized graphene/GCE (50.0 nM) [40]. In addition, the GR-β-CD/CuO NPs composite modified electrode shows wider linear response range and appropriate R^2 when compared to previously reported modified electrodes for determination of MTZ [27–30,37–41]. The result reveals that the GR-β-CD/CuO NPs composite can be used as an advance electrode material for low-level detection of MTZ.

3.5. Operational stability and selectivity of the sensor

The operational stability of the GR-β-CD/CuO NPs composite modified RDE for detection of 500 nM MTZ was evaluated using amperometry. Fig. 7C shows the amperometric response of GR-β-CD/CuO NPs composite modified RDE for the addition of 500 nM MTZ (curve a and b) into the constantly stirred pH 7.0 and its related current response up to 2000 s. Other experimental conditions are similar to Fig. 7A. It can be seen that a sharp amperometric i-t response was observed for addition of 500 nM MTZ, and the current response was almost unchanged up to 2000 s. The result indicates that the excellent operational stability of the sensor. Selectivity of the electrode is more important to use for the practical applications, hence the GR-β-CD/CuO NPs composite modified RDE was evaluated for detection of 50 nM MTZ in the presence of 20 folds (1.0 μM) addition of potentially active different interfering species. The amperometric i-t was used to evaluate the selectivity of the sensor, and the experimental conditions are similar to Fig. 7A. We have chosen a mixed range of interfering compounds such as nitro compounds (nitrobenzene and 4-nitrophenol), drugs (nilutamide and flutamide), amino acids, neurotransmitters, and sugars. The obtained selectivity results of the sensor are shown in Fig. 7D. It can be seen that the 20 folds addition of interference above compounds did not show any apparent response on GR-β-CD/CuO NPs composite modified RDE. However, a clear and well-defined amperometric response was observed for the addition of 50 nM MTZ. The high selectivity is possibly due to the lower working potential (−0.6 V) of the sensor than the tested interfering

Table 1
Analytical comparison of GR–β-CD/CuO NPs composite sensor with the previously reported sensors for the determination of MTZ.

Sensor electrode	Detection method	R^2	LOD[a] (nM)	Linear range (μM)	Ref.
[1]Chit/CuTsPc/GCE	DPV[b]	0.9976	0.41	0.008–0.72	[28]
[2]MWCNTs/CTS-Ni/GCE	DPV	0.0999	25.0	0.1–150.0	[29]
[3]Gr-IL/GCE	DPV	0.9990	47.0	0.1–25.0	[30]
[4]AGCE	DPV	0.997	1100.0	2.0–600.0	[37]
[5]MWCNT/GCE	DPV	0.997	6.0	0.25–10.0	[38]
[6]SWCNT/GCE	Amperometry	0.9989	63.0	0.1–200.0	[39]
[7]P-AuE	LSV[c]	0.9950	150.0	0.5–10.0	[40]
[8]AgNPs/SF-GR/GCE	DPSV[d]	0.9993	50.0	0.1–20.0	[41]
GR–β-CD/CuO NPs/GCE	Amperometry	0.9969	0.6	0.002–210.0	This work

[a] Limit of detection.
[b] Differential pulse voltammetry.
[c] Linear sweep voltammetry.
[d] Differential pulse stripping voltammetry.
[1] Chitosan protected tetrasulfonated copper phthalocyanine thin-film modified glassy carbon electrode.
[2] Multi-walled carbon nanotubes and chitosan-nickel complex modified glassy carbon electrode.
[3] Graphene and ionic liquid (1-butyl-3-methylimidazolium hexafluorophosphate) composite modified glassy carbon electrode.
[4] Activated glassy carbon electrode.
[5] Multi-walled carbon nanotube modified glassy carbon electrode.
[6] Single wall carbon nanotubes modified glassy carbon electrode.
[7] Pretreated gold electrode.
[8] Silver nanoparticles/sulfonate functionalized graphene modified glassy carbon electrode.

Table 2
Determination of MTZ in pharmaceutical tablets using GR-β-CD/CuO NPs composite. RSD is relative to the 3 measurements.

Sample	Added (μM)	Found (μM)	Recovery (%)	RSD (%)
A	50.0	49.2	98.4	2.1
B	100.0	97.6	97.6	2.6
C	150.0	146.3	97.5	1.7

compounds. The result authenticates that the GR-β-CD/CuO NPs composite modified electrode can be used for the selective detection of MTZ.

3.6. Determination of MTZ in pharmaceutical tablets

To evaluate the practical feasibility sensor, the GR-β-CD/CuO NPs composite was used for the determination of MTZ in MTZ containing pharmaceutical tablets (400 mg). Amperometric *i-t* method was used for the real sample analysis and standard addition method was used for the calculation of recovery of MTZ in pharmaceutical tablets. The desired concentration of MTZ tablet samples (stock solution) was prepared using pH 7.0. A known concentration MTZ containing tablet samples was used for real sample analysis. The obtained recovery values of MTZ in pharmaceutical tablets are summarized in Table 2. It can be seen that the average recovery of MTZ in the real samples was 97.8% with the relative standard deviation (RSD) of 2.1% (3 measurements). The results indicate that the GR-β-CD/CuO NPs composite modified electrode can be used for the precise practical determination of MTZ in real samples. The reusability of the GR-β-CD/CuO NPs composite sensor was tested using cyclic voltammetry. The fabricated sensor was tested in 8 set of pH 7.0 containing 50 μM MTZ samples at a scan rate of 50 mV/s. The other experimental conditions are similar to Fig. 4A. The sensor shows the RSD of 2.9% for detection of 8 different MTZ containing pH 7.0 samples. The result indicates that the high reusability of the GR-β-CD/CuO NPs composite modified electrode towards the detection of MTZ.

4. Conclusions

In conclusion, a simple amperometric electrochemical sensor was fabricated using GR-β-CD/CuO NPs composite modified electrode. The physicochemical characterizations confirmed the successful formation of GR-β-CD CuO NPs composite and the existence of few-layered GR domains. Under optimized conditions, the fabricated sensor showed a wider linear range for the detection of MTZ with a lower LOD of 0.6 nM. The sensor showed advanced analytical performances towards detection of MTZ than previously reported GR and carbon nanomaterials based MTZ sensors. The sensor was highly selective and successfully applied for the practical determination of MTZ in pharmaceutical tablets. The discussed analytical features of the sensor authenticate that the sensor can be used for the real-time detection of MTZ in pharmaceutical and biological samples. As a future perspective, the synthesized GR-β-CD/CuO NPs composite could be used for fabrication of other electrochemical sensors and biosensors.

Conflicts of interest

We confirm that there are no conflicts to declare.

Acknowledgments

The work was supported by the Engineering and Materials Research Centre (EMRC), School of Engineering, Manchester Metropolitan University, Manchester, UK. This work also jointly sponsored by the Ministry of Science and Technology (project No: 106-2119-M-027-001) of Taiwan. Authors also acknowledge the Precision analysis and Materials Research Center, National Taipei University of Technology for providing the all necessary Instrument facilities.

References

[1] X. Huang, X. Qi, Graphene-based composites, Chem. Soc. Rev. 41 (2012) 666–686.
[2] E.P. Randviir, D.A.C. Brownson, C.E. Banks, A decade of graphene research: production, applications and outlook, Mater. Today 17 (2014) 426–432.
[3] W. Choi, I. Lahiri, R. Seelaboyina, Y.S. Kang, Synthesis of graphene and its applications: a review, Crit. Rev. Solid State Mater. Sci. 35 (2010) 52–71.
[4] B. Unnikrishnan, S. Palanisamy, S.M. Chen, A simple electrochemical approach to fabricate a glucose biosensor based on graphene-glucose oxidase biocomposite, Biosens. Bioelectron. 39 (2013) 70–75.
[5] T.B. Sarfraj, H. Mujawara, Q.T.T. Swapnil, B.A. Dai, S. Lee, W. Lee, S.H. Han, S.H. Lee, Graphene/carbon nanotubes composites as a counter electrode for dye-sensitized solar cells, Curr. Appl Phys. 12 (2012) e49–e53.

[6] L. Song, C. Guo, T. Li, S. Zhang, C60/graphene/g-C_3N_4 composite photocatalyst and mutually- reinforcing synergy to improve hydrogen production in splitting water under visible light radiation, Ceram. Int. 43 (2017) 7901–7909.
[7] Q. Zhuo, Y. Ma, J. Gao, P. Zhang, Y. Xia, Y. Tian, X. Sun, J. Zhong, X. Sun, Facile synthesis of graphene/metal nanoparticle composites via self-catalysis reduction at room temperature, Inorg. Chem. 52 (2013) 3141–3147.
[8] S. Zhang, Y. Shao, H. Liao, J. Liu, I.A. Aksay, G. Yin, Y. Lin, Graphene decorated with PtAu alloy nanoparticles: facile synthesis and promising application for formic acid oxidation, Chem. Mater. 23 (2011) 1079–1081.
[9] Y. Guo, S. Guo, J. Ren, Y. Zhai, S. Dong, E. Wang, Cyclodextrin functionalized graphene nanosheets with high supramolecular recognition capability: synthesis and host–guest inclusion for enhanced electrochemical performance, ACS Nano 4 (2010) 4001–4010.
[10] P. Mahala, A. Kumar, S. Nayak, S. Behura, C. Dhanavantri, O. Jani, Graphene, conducting polymer and their composites as transparent and current spreading electrode in GaN solar cells, Superlattices Microstruct. 92 (2016) 366–373.
[11] H. Gómez, M.K. Ram, F. Alvi, P. Villalba, E. Stefanakos, A. Kumar, Graphene-conducting polymer nanocomposite as novel electrode for supercapacitors, J. Power Sources 196 (2011) 4102–4108.
[12] X. Wu, Y. Xing, D. Pierce, J.X. Zhao, One-pot synthesis of reduced graphene oxide/metal (oxide) composites, ACS Appl. Mater. Interfaces 9 (2017) 37962–37971.
[13] S.H. Choi, J.K. Lee, Y.C. Kang, Three-dimensional porous graphene-metal oxide composite microspheres: preparation and application in Li-ion batteries, Nano Res. 8 (2015) 1584–1594.
[14] Vellaichamy Balakumar, Periakaruppan Prakash, A facile in situ synthesis of highly active and reusable ternary Ag-PPy-GO nanocomposite for catalytic oxidation of hydroquinone in aqueous solution, J. Catal. 344 (2016) 795–805.
[15] Vellaichamy Balakumar, Periakaruppan Prakash, Silver nanoparticle-embedded RGO-nanosponge for superior catalytic activity towards 4-nitrophenol reduction, RSC Adv. 6 (2016) 88837–88845.
[16] Vellaichamy Balakumar, Periakaruppan Prakash, A facile, one-pot and eco-friendly synthesis of gold/silver nanobimetallics smartened rGO for enhanced catalytic reduction of hexavalent chromium, RSC Adv. 6 (2016) 57380–57388.
[17] B. Vellaichamy, P. Periakaruppan, S.K. Ponnaiah, A new in-situ synthesized ternary CuNPs-PANI-GO nano composite for selective detection of carcinogenic hydrazine, Sensors Actuat. B 245 (2017) 156–165.
[18] B. Vellaichamy, S.K. Ponnaiah, P. Periakaruppan, An in-situ synthesis of novel Au@NG-PPy nanocomposite for enhanced electrocatalytic activity toward selective and sensitive sensing of catechol in natural samples, Sensors Actuat. B 253 (2017) 392–399.
[19] S. Palanisamy, K. Thangavelu, S.M. Chen, V. Velusamy, M.H. Chang, T.W. Chen, F.M.A. Hemaid, M.A. Ali, S.K. Ramaraj, Synthesis and characterization of polypyrrole decorated graphene/β-cyclodextrin composite for low level electrochemical detection of mercury (II) in water, Sens. Actuat., B 243 (2017) 888–894.
[20] G. Liu, B. Zheng, Y. Jiang, Y. Cai, J. Du, H. Yuan, D. Xiao, Improvement of sensitive CuO NFs–ITO nonenzymatic glucose sensor based on in situ electrospun fiber, Talanta 101 (2012) 24–31.
[21] X. Xiao, M. Wang, H. Li, Y. Pan, P. Si, Non-enzymatic glucose sensors based on controllable nanoporous gold/copper oxide nanohybrids, Talanta 125 (2014) 366–371.
[22] K.J. Choi, H.W. Jang, one-dimensional oxide nanostructures as gas-sensing materials: review, Sensors 10 (2010) 4083–4099.
[23] Y.Y. Yu, R.X. Xu, C. Gao, T. Luo, Y. Jia, J.H. Liu, X.J. Huang, novel 3D hierarchical cotton-candy-like CuO: surfactant-free solvothermal synthesis and application in As(III) removal, ACS Appl. Mater. Interfaces 4 (2012) 1954–1962.
[24] J. Liu, J. Jin, Z. Deng, S.Z. Huang, Z.Y. Hu, L. Wang, C. Wang, L.H. Chen, Y. Li, G.V. Tendeloo, B.L.J. Su, Tailoring CuO nanostructures for enhanced photocatalytic property, J. Colloid Interface Sci. 384 (2012) 1–9.
[25] N.C. Desai, A.S. Maheta, K.M. Rajpara, V.V. Joshi, H.V. Vaghani, H.M. Satodiya, Green synthesis of novel quinoline based imidazole derivatives and evaluation of their antimicrobial activity, J. Saudi Chem. Soc. 18 (2014) 963–971.
[26] A.H. Davies, J.A. Mafadzean, S. Squires, Treatment of vincent's stomatitis with metronidazole, Br. Med. J. 1 (1964) 1149.
[27] Y. Gu, X. Yan, C. Li, B. Zheng, Y. Li, W. Liu, Z. Zhang, Biomimetic sensor based on molecularly imprinted polymer with nitroreductase-like activity for metronidazole detection, Biosens. Bioelectron. 77 (2016) 393–399.
[28] S. Meenakshi, K. Pandian, L.S. Jayakumari, S. Inbasekaran, Enhanced amperometric detection of metronidazole in drug formulations and urine samples based on chitosan protected tetrasulfonated copper phthalocyanine thin-film modified glassy carbon electrode, Mater. Sci. Eng., C 59 (2016) 136–144.
[29] A. Mao, H. Li, L. Yu, X. Hu, Electrochemical sensor based on multi-walled carbon nanotubes and chitosan-nickel complex for sensitive determination of metronidazole, J. Electroanal. Chem. 799 (2017) 257–262.
[30] J. Peng, C. Hou, X. Hu, Determination of metronidazole in pharmaceutical dosage forms based on reduction at graphene and ionic liquid composite film modified electrode, Sens. Actuat., B 169 (2012) 81–87.
[31] T.W. Chen, S. Palanisamy, S.M. Chen, V. Velusamy, K.K. Ramasubbu, S.K. Ramaraj, A novel non-enzymatic glucose sensor based on melamine supported CuO nanoflakes modified electrode, Adv. Mater. Lett. 8 (2017) 852–856.
[32] Z.S. Wu, W. Ren, D.W. Wang, F. Li, B. Liu, H.M. Cheng, High-energy MnO_2 nanowire/graphene and graphene asymmetric electrochemical capacitors, ACS Nano 4 (2010) 5835–5842.
[33] L. Xu, C. Srinivasakannan, J. Peng, L. Zhang, D. Zhang, Synthesis of Cu-CuO nanocomposite in microreactor and its application to photocatalytic degradation, J. Alloys Compd. 695 (2017) 263–269.
[34] S. Palanisamy, P.Y. Fan, S.M. Chen, V. Velusamy, J.M. Hall, Facile preparation of a cellulose microfibers–exfoliated graphite composite: a robust sensor for determining dopamine in biological samples, Cellulose 24 (2017) 4291–4302.
[35] D.A.C. Brownson, S.A. Varey, F. Hussain, S.J. Haigh, C.E. Banks, Electrochemical properties of CVD grown pristine graphene: monolayer- vs. quasi-graphene, Nanoscale 6 (2014) 1607–1621.
[36] S. Palanisamy, T. Kokulnathan, S.M. Chen, V. Velusamy, S.K. Ramaraj, Voltammetric determination of Sudan I in food samples based on platinum nanoparticles decorated on graphene-β-cyclodextrin modified electrode, J. Electroanal. Chem. 794 (2017) 64–70.
[37] A. Ozkan, Y. Ozkan, Z. Senturk, Electrochemical reduction of metronidazole at activated glassy carbon electrode and its determination in pharmaceutical dosage forms, J. Pharm. Biomed. Anal. 17 (1998) 299–305.
[38] S. Lü, K. Wu, X. Dang, S. Hu, Electrochemical reduction and voltammetric determination of metronidazole at a nanomaterial thin film coated glassy carbon electrode, Talanta 63 (2004) 653–657.
[39] A. Salimi, M. Izadi, R. Hallaj, M. Rashidi, Simultaneous determination of ranitidine and metronidazole at glassy carbon electrode modified with single wall carbon nanotubes, Electroanalysis 19 (2007) 1668–1676.
[40] A. Rezaei, S. Damiri, Fabrication of a nanostructure thin film on the gold electrode using continuous pulsed-potential technique and its application for the electrocatalytic determination of metronidazole, Electrochim. Acta 55 (2010) 1801–1808.
[41] H.Y. Zhai, Z.X. Liang, Z.G. Chen, Simultaneous detection of metronidazole and chloramphenicol by differential pulse stripping voltammetry using a silver nanoparticles/sulfonate functionalized graphene modified glassy carbon electrode, Electrochim. Acta 171 (2015) 105–113.